Two-electron quantum disks

F. M. Peeters* and V. A. Schweigert†
Departement Natuurkunde, Universiteit Antwerpen (UIA), Universiteitsplein 1, B-2610 Antwerpen, Belgium
(Received 31 May 1995)

The energy levels of a quantum disk containing one or two electrons are calculated as a function of an external magnetic field. The confinement potential is a hard wall of finite height. The cyclotron transition energies are investigated and the effect of the finite width of the disk on the Coulomb energy is studied. Our results are applied to the $In_xGa_{1-x}As/GaAs$ dots and agree well with experiment.

I. INTRODUCTION

Quantum dots are structures in which the charge carriers (electrons or holes) are confined in all three dimensions.[1,2] Due to the singular nature (δ-function-like) of their density of states, they are interesting for optoelectronic device applications. From the fundamental physics point of view, they are like artificial atoms in which the number of electrons can be increased almost unlimited and in a controlled way.

Usually, those dot structures are created experimentally by applying lithographic or etching techniques to impose a lateral structure to an otherwise two-dimensional (2D) electron system. The dot structures[2] in this manner are mainly determined by surface effects, process induced damage, and rough heterostructure interfaces. For optoelectronic applications, high quantum efficiency, strong confinement, and spatial homogeneity are required. In search for defect-free structures of high optical quality, alternative techniques have been developed, which form quantum sized structures directly during the growth.

Self-organized growth is recognized to be a very promising technique for obtaining well defined high mobility nanostructures, because it leads inherently to a low density of defects, as compared to the density of defects introduced usually with lithographic methods. Self-organized growth of $In_xGa_{1-x}As$ quantum dots has been reported using molecular beam epitaxy,[3] metal-organic vapor-phase epitaxy,[4] and metal-organic chemical vapor deposition.[5] The dots were covered with GaAs. Dots of a diameter down to 12 nm have been realized experimentally. Similar nanometer-scale quantum dots have been realized[6] with InAs on GaAs(001), but in this case, the dots are pyramid shaped.

It was found experimentally that the $In_xGa_{1-x}As$ dots are remarkably uniform in size, with their diameter fluctuating by only about 10% and their thickness, which can be as thin as a few monolayers, fluctuating by only a single monolayer.[7] Lateral diameters of $d=20$ nm (Ref. 8) down to $d=13$ nm (Ref. 7) have been realized with a dot thickness of the order of $L_z \approx 2.5$ nm. This resulted in large interlevel spacings of 30–40 meV between the ground state and the first excited state, which should be compared with only a few meV for typical parabolic quantum dots.

In contrast to the electrostatically defined dots in which the confinement potential can often be approximated by a parabolic potential, these structures have a hard-wall confinement potential that is induced by the discontinuity of the conduction band at the edge of the dot. This is similar to the band discontinuity in quantum wells. Parabolic confinement has the property that the magneto-optical response of the system is solely due to the response of the center of mass motion of the system. This is a consequence of a generalized Kohn's theorem.[9] Coupling with the other degrees of freedom is possible by adding band nonparabolicity[10] to the electron conduction band or adding a nonparabolic component to the confinement.[11] In the case of a hard-wall confinement,[12] the center of mass motion can no longer be separated out and radiation will couple to more degrees of freedom. As a consequence, a much richer magneto-optical spectrum is expected.

In the present work, we have investigated the energy levels of a quantum disk with a hard-wall (of finite height) confinement in the presence of an external perpendicular magnetic field. Previous work on hard-wall confinement was restricted to the one-electron energy spectrum and to the extreme case of an infinite height confinement wall. For example, circular dots were considered in an arbitrary magnetic field[12] and square-shaped dots at a zero magnetic field.[13] Here, we will study the Coulomb interaction between two electrons, which are confined by a hard-wall circular potential of finite height and nonzero thickness. For our numerical analysis of the problem, we have the $In_xGa_{1-x}As/GaAs$ quantum disks in mind.

The paper is organized as follows. In Sec. II, we present the theoretical model and explain our method of solution. The numerical results for the two-electron energy spectrum are presented in Sec. III. In Sec. IV, we compare our results with the cyclotron resonance data of Ref. 8 and investigate the effect of the finite width of the quantum disk on the contribution of the Coulomb energy to the position of the transition energy.

II. THEORETICAL MODEL

The Hamiltonian describing our system is given by

$$H=\sum_{j=1}^{2}\left(\vec{p}_j-\frac{e}{c}\vec{A}_j\right)\frac{1}{2m(\vec{r})}\left(\vec{p}_j-\frac{e}{c}\vec{A}_j\right)+V_c(\vec{r}_1-\vec{r}_2)+\sum_{j=1}^{2}V(\vec{r}_j), \tag{1}$$

where $V(\rho,z)=0$ ($\rho<R, |z|<L_z$), V_0 (otherwise) is the confinement potential with R the radius of the quantum disk and L_z its thickness, $\vec{r}=(\rho,z)$ with $\rho=\sqrt{x^2+y^2}$, and $V_c(\vec{r})=e^2/4\pi\epsilon|\vec{r}|$ is the Coulomb potential between the two electrons. We allow for a difference in electron mass between the dot region and the region outside the dot: $m(\vec{r})=m_w$ inside the disk and m_b outside the disk.

For the experimental system of $In_xGa_{1-x}As/GaAs$ disks, one has $x\approx 0.5$. For $In_xGa_{1-x}As$, we took the physical parameters for an indium concentration of $x=0.53$, which are well known, due to the fact that this material has the same lattice parameter as InP and has been investigated very intensively for possible optical applications. In GaAs, the electrons have an effective mass $m^*/m_0=0.067$, the static dielectric constant is $\epsilon_0=12.5$ and the band gap is $E_g=1.519$ eV at helium temperature. For $In_{0.53}Ga_{0.47}As$, we have $m^*/m_0=0.041$, $\epsilon_0=13.8$, and a band gap of $E_g=0.813$ eV. This results in a band gap difference of $\Delta E_g=706$ meV between GaAs and $In_xGa_{1-x}As$, which leads to a conduction-band offset[14] of about $\Delta E_c=500$ meV $=V_0$. In the numerical calculation, we included the mass difference between the two materials, but we assumed $\epsilon_0=13.8$ thoughout the whole system, which is expected to be a reasonable approximation.

We assume that only the lowest electronic subband in the z direction is occupied and that there is no coupling between the z direction and the (x,y) plane,[15] which is satisfied in the systems under investigation, because of the much stronger confinement along the z direction as compared to the (x,y) direction. In the Appendix we argue that the above 3D problem for the system under consideration with $L_z\approx 2.5$ nm and $R\geqslant 10$ nm can accurately be approximated by a 2D problem in which the effective mass in the $In_xGa_{1-x}As$ region is replaced by $m^*/m_0\approx 0.0465$ and the barrier height by $V_0\approx 245$ meV. This renormalization of the parameters is a consequence of the finite penetration of the electron wave function into the GaAs region. In fact, the Coulomb potential should also be altered. This was done by replacing the Coulomb repulsion by $V_c(\rho)=e^2/4\pi\epsilon\sqrt{\rho^2+\lambda^2}$, where in Ref. 16 it was found that $\lambda\approx 0.2L_z$ for a quantum well of width L_z.

Thus, the Hamiltonian describing our two-electron system is given by the effective Hamiltonian, which describes motion in 2D,

$$H'=H(\vec{\rho}_1)+H(\vec{\rho}_2)+V_c(\vec{\rho}_1-\vec{\rho}_2), \tag{2}$$

where $V_c(\rho)=e^2/4\pi\epsilon\sqrt{\rho^2+\lambda^2}$ is the Coulomb repulsion between the two electrons. Because of the cylinder symmetry of the problem, we use cylindrical coordinates (ρ,ϕ) and the vector potential will be taken in the symmetric gauge $\vec{A}=\frac{1}{2}B\rho\vec{e}_\phi$. The Schrödinger equation for the one-electron problem is now given by

$$\left\{-\frac{\hbar^2}{2}\left[\frac{1}{\rho}\frac{\partial}{\partial\rho}\left(\frac{\rho}{m(\rho)}\frac{\partial}{\partial\rho}\right)+\frac{1}{m(\rho)\rho^2}\frac{\partial^2}{\partial\phi^2}\right]-\frac{i}{2}\hbar\omega_c\frac{\partial}{\partial\phi}+\frac{1}{8}m\omega_c^2\rho^2+V(\rho)\right\}\Psi(\rho,\phi)=E\Psi(\rho,\phi), \tag{3}$$

where $\omega_c=eB/mc$ is the cyclotron frequency. The one-electron wave function is separable, $\Psi(\rho,\phi)=(1/\sqrt{2\pi})\,e^{il\phi}R_l(\rho)$, where $l=0,\pm 1,\pm 2,\ldots$ is the angular momentum, and the radial part of the wave function $R_l(\rho)$ is described by the following equation:

$$\left[-\frac{\hbar^2}{2r}\frac{\partial}{\partial\rho}\left(\frac{\rho}{m(\rho)}\frac{\partial}{\partial\rho}\right)+\frac{\hbar^2 l^2}{2m(\rho)\rho^2}+\frac{l}{2}\hbar\omega_c+\frac{1}{8}m\omega_c^2\rho^2+V(\rho)\right]R_l(\rho)=ER_l(\rho). \tag{4}$$

For the hard-wall problem with $V_0=\infty$, the energy spectrum of the single-electron problem was solved in Ref. 12 where it was found that the radial part of the wave function is a linear combination of confluent hypergeometric functions. Here, we found it more convenient to use the nonuniform space grid (ρ_j, $j=1,\ldots,j_s$) in order to solve Eq. (4) numerically. Let $\zeta_j^l=h_jR_l(\rho_j)$, where $h_j=\sqrt{(\rho_{j+1/2}^2-\rho_{j-1/2}^2)/2}$, $\rho_{j+1/2}=(\rho_{j+1}+\rho_j)/2$ for $j=1,\ldots,j_s-1$, $\rho_{1/2}=\rho_1$, $\rho_{j_s+1/2}=\rho_{j_s}=R_s$, R_s is the right boundary of the considered region, which is larger than R. Within this finite difference scheme, Eq. (4) can be written in the following form:

$$\sum_j A_{i,j}^l\zeta_j^l=E\zeta_i^l, \tag{5}$$

where all the matrix elements $A_{i,j}$ are equal to zero, except the diagonal and off-diagonal components,

$$A_{j,j}^l=\frac{\hbar^2(\mu_{j+1}+\mu_j)}{2h_j^2}+\frac{\hbar^2l^2}{2m(\rho_j)\rho_j^2}+\frac{l}{2}\hbar\omega_c+\frac{1}{8}m\omega_c^2\rho_j^2+V(\rho_j),$$

$$A_{j,j+1}^l=-\frac{\hbar^2\mu_{j+1}}{2h_jh_{j+1}},\quad A_{j,j-1}^l=A_{j-1,j}^l,$$

where we introduced the notation

$$\mu_j=\frac{1}{2(\rho_j-\rho_{j-1})}\left(\frac{\rho_j}{m(\rho_j)}+\frac{\rho_{j-1}}{m(\rho_{j-1})}\right),$$

for $j=2,\ldots,j_s$ and $\mu_1=\mu_{j_s+1}=0$. The above scheme is accurate to $O(h^2)$. The condition $\mu_{j_s+1}=0$ is equivalent to taking the first derivative of the wave function equal to zero on the right boundary of the space grid, which is situated far in the barrier region $R_s=(2-3)R$. For the nonzero angular momentum values, the boundary condition $R_l(0)=0$ is used on the left boundary of the space grid, which results in $A_{1,i}^{l\neq 0}=\delta_{1,i}$, where $\delta_{i,j}$ is the unit matrix. The matrix $A_{i,j}^l$ is symmetrical and positive defined. Using the commonly accepted Hausholder diagonalization technique for the matrix A, we obtain the eigenvalues E_{nl} and eigenvectors $\zeta_{nl,j}$ of the matrix A^l for different values of the angular momentum.

The two-electron wave functions with fixed total momentum L are constructed as being linear combinations of these one-electron wave functions:

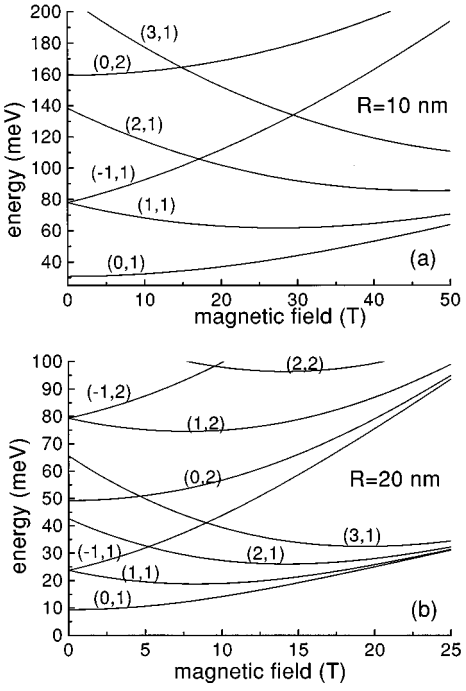

FIG. 1. The one-electron levels of an $In_xGa_{1-x}As$ disk of thickness $L_z=2.5$ nm and radius (a) $R=10$ nm and (b) $R=20$ nm, which is embedded in GaAs. The different energy levels are indicated by their corresponding quantum numbers (l,n).

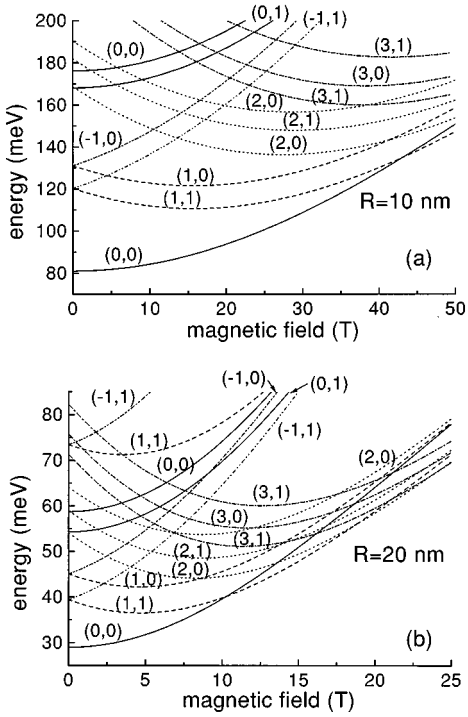

FIG. 2. The same as Fig. 1, but now for a disk containing two electrons. The levels are labeled by (L,S), where L is the total angular momentum and S is the total spin. Levels having the same L are plotted using the same type of curve.

$$\Psi(\vec{\rho}_1,\vec{\rho}_2)=\sum_{k=1}^{k=k_m}\sum_{n=1}^{n=k_m}\sum_{l=-l_m}^{l=l_m}{}'C_{kn}^{l}R_{k,(L+l)/2}(\rho_1)\times R_{n,(L-l)/2}(\rho_2)e^{i1/2\,(\phi_1-\phi_2)+i\,L/2\,(\phi_1+\phi_2)}, \tag{6}$$

where the subscripts k and n correspond to the energy levels of the one-electron problem. The sum Σ' denotes that only even values of the angular momentum l are taken when L is even and odd values otherwise. The matrix elements of Hamiltonian (2) are found using the same space grid as for the radial functions. Then eigenenergies and eigenvectors are calculated using the Hausholder technique, for different values of the total momentum L. We checked the accuracy of our method by comparing our results with those of Ref. 11 for parabolic confinement. For most of our numerical results, we used $k_m=10$, $l_m=10$ in Eq. (6), which leads to an accuracy for the ground state energy better than 1%. Furthermore, our numerical results also satisfy the following exact symmetry, relation $C_{kn}^{l}=\pm C_{kn}^{-l}$, where the plus sign corresponds to the singlet state with total spin $S=0$, and the minus sign to the triplet state with $S=1$. Because the spatial and spin parts of the wave function decouple, the value of the total spin of the system will determine the symmetry of the spatial wave function under particle permutation. Furthermore, the system has rotational symmetry, which implies that the total angular momentum L is a conserved quantity. The two-electron states are indicated by the quantum numbers (L,S,N), which correspond to the Nth energy state with total angular momentum L and total spin S.

III. THE ENERGY SPECTRUM

We calculated the energy spectra of the one- (Fig. 1) and the two- (Fig. 2) electron systems as a function of the magnetic field. Two different values of the radius of the quantum dot, (a) $R=10$ nm and (b) $R=20$ nm, are considered. The single-electron energy levels are labeled by the quantum numbers (l,n). When we compare the energy spectra with the one of a parabolic quantum dot, we notice the following: (1) the states with (l,n) and $(-l,n)$ are degenerate at $B=0$, similar to the parabolic dot problem, which is directly related to the cylindrical symmetry of the dot; (2) for large magnetic fields, i.e., $B\to\infty$, the energy levels approach $(n-1/2)\hbar\omega_c$ when $l\geqslant 0$ and $(n+|l|-1/2)\hbar\omega_c$ when $l\leqslant 0$, which is similar to the parabolic dot system. For a smaller radius of the dot [Fig. 1(b)], a larger magnetic field is needed to reach these limits. In fact, the quantity $\hbar\omega_c/(\hbar^2/mR^2)$ is the one that we should consider when comparing the magnetic field dependence of dots with different radii; (3) the separation between the different energy levels for $B=0$ is not equidistant as in the parabolic dot problem.

The energy levels for the two-electron hard-wall dot are shown in Fig. 2, where we labeled them by (L,S), with L the total angular momentum and S the total spin. Energy levels with the same total angular momentum are drawn using the same type of curve. Note that as a function of the magnetic field, the ground state exhibits a transition from the singlet to the triplet state. This is similar to the case for parabolic confined dots. For disks with a small radius, a much larger magnetic field is needed for such a transition. It occurs at $B\approx 10,19,24$ T for $R=20$ nm and $B\approx 43$ T for $R=10$ nm. The latter is a factor of 4 larger than the one for $R=20$ nm,

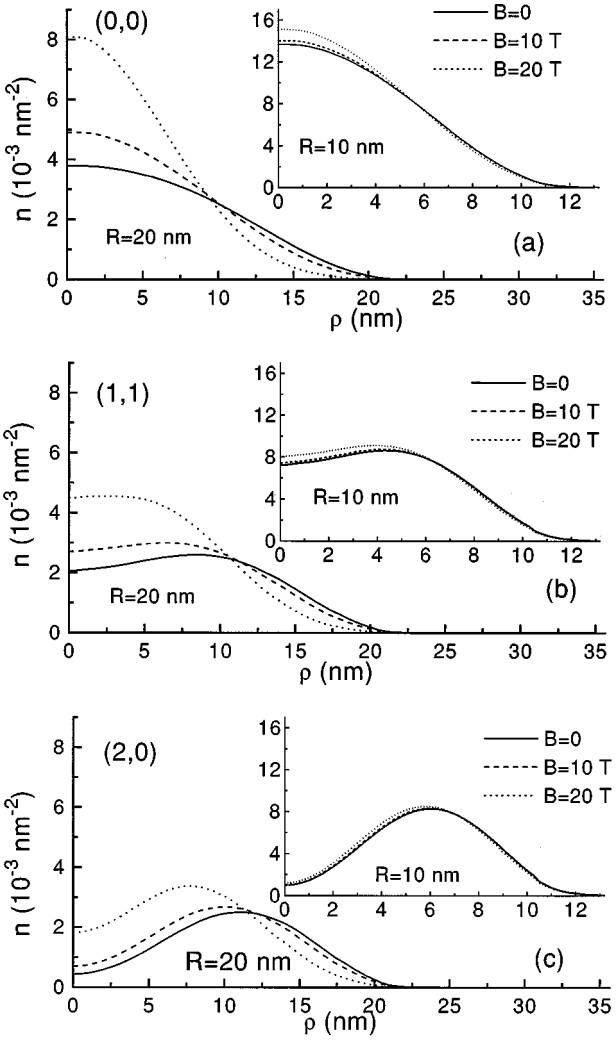

FIG. 3. The radial electron density for the disks of Fig. 1 containing two electrons. We give results for the following three states: (a) the singlet $(L,S)=(0,0)$, (b) the triplet (1,0), and (c) the singlet (2,0), and for three values of the magnetic field $B=0$, 10, 20 T.

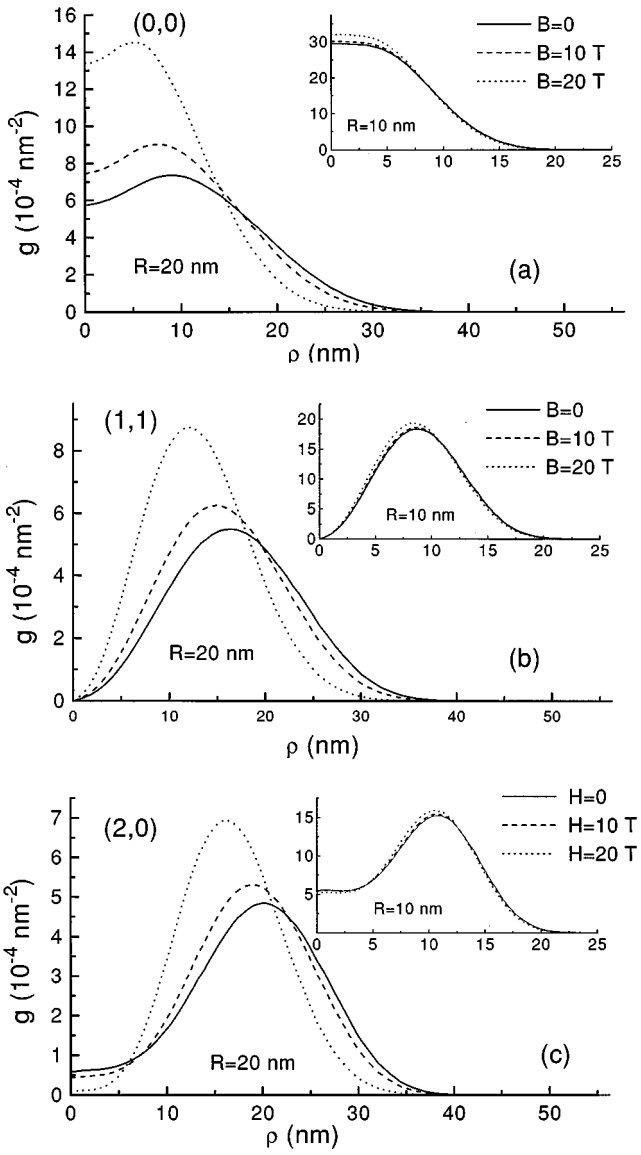

FIG. 4. The same as Fig. 3, but now for the pair correlation function.

which is due to the fact that the confinement energy ($\sim R^2$) is 4 times larger. At this transition, the total angular momentum of the ground state changes, i.e., it increases. These are the so-called *magic number* ground state transitions, which are a result of the competition between the single-electron confinement energy and the many body electron-electron interactions.[17] Such magnetic field induced angular momentum (and spin) transitions have been observed experimentally,[18] for dots with paraboliclike confinement.

The electron density, which is defined by

$$n(\rho)=\sum_{i=1}^{2}\langle\delta(\vec{\rho}-\vec{\rho}_i)\rangle,$$

is shown in Fig. 3 for disks containing two electrons and for two values of the radius of the disk, $R=20$ nm and $R=10$ nm (insets of figures), and three values of the external magnetic field $B=0$, 10, and 20 T, and for three different states of the system: (a) singlet $L=0$, $S=0$, (b) triplet $L=1$, $S=1$, and (c) singlet $L=2$, $S=0$. Notice that (1) for $\rho>R$ there is almost no leakage of the wave function into the barrier, which is due to the large barrier height of $V_0=245$ meV in the present system. Only for the smallest disk, $R=10$ nm, is there some penetration into the GaAs material; (2) the effect of the magnetic field on the electron density is very small for the disk with $R=10$ nm; and (3) with increasing magnetic field the electrons are pulled closer towards the center of the disk.

The pair correlation function $g(\vec{r})$ defined by

$$g(\vec{\rho})=\langle\delta(\vec{\rho}-\vec{\rho}_1+\vec{\rho}_2)\rangle \tag{7}$$

indicates the correlation between the electrons and gives the probability to find two electrons at a distance $\rho=|\rho|$ from each other. This function is shown in Fig. 4 for our disk system containing two electrons and for the same parameters as in Fig. 3. Note that this function depends very strongly on the state of the system; the $\rho\sim 0$ behavior is most sensitive. With increasing magnetic field, the electrons can approach each other much more closely, which is consistent with the electron density behavior of Fig. 3. Notice that in the

singlet state the pair correlation function for the $R=10$ nm dot is ρ independent for $|\rho|\leqslant 5$ nm while for the larger dot of $R=20$ nm, the electron repulsion leads to a maximum near $\rho\sim 8$ nm ($B=10$ T), which indicates that the electron probability distribution is barbell shaped.

IV. CYCLOTRON RESONANCE TRANSITIONS

In cyclotron resonance experiments, transitions are invoked between the ground state and excited states. In the present case of hard-wall confinement the selection rule on the change of angular momentum $\Delta L=\pm 1$ is still fulfilled, but there are no other selection rules. For parabolic quantum dots, we know that the other quantum number must satisfy the selection rule: $\Delta N=0,1$. The selection rules on ΔL and ΔN for parabolic quantum dots are responsible for the fact that only two transition energies are possible:[19] $\Delta E_{\pm}=\frac{1}{2}\hbar\omega\pm\frac{1}{2}\hbar\omega_c$ with $\omega=\sqrt{\omega_c^2+4\omega_0^2}$, where ω_0 is the confinement frequency. In the present system under study, more transitions are possible.[20] This is apparent when we calculate the oscillator strength for dipole transitions, which is defined by

$$F_{i,f}=\frac{2m}{\hbar^2}(E_f-E_i)\left|\left\langle \Psi_i\left|\sum_{j=1}^{2}\frac{1}{2}r_j e^{\pm i\phi_j}\right|\Psi_f\right\rangle\right|^2, \quad (8)$$

where Ψ_i is the initial state with energy E_i and Ψ_f the final state after the transition with energy E_f. The f-sum rule tells us that we must have $\Sigma_f F_{i,f}=1$.

Some of the possible transition energies $\Delta E=E_f-E_i$ for a quantum disk with one electron and radius $R=10$ nm (full curves) and $R=20$ nm (dashed curves) are shown in Fig. 5(a). The corresponding oscillator strengths are given in Fig. 5(b). Although more transitions are possible, we still find that the $\Delta n=1$ transitions have the largest oscillator strength. The next transition has $\Delta n=2$ and exhibits an oscillator strength which is about a factor of 50 smaller.

The results for the two-electron system are depicted in Fig. 6 for (a) $R=10$ nm and (b) $R=20$ nm. The possible transitions are labeled by the final states (L,S,N). The discontinuities in the two-electron spectrum at $B\approx 10$ T and $B\approx 19$ T for $R=20$ nm and at $B\approx 43$ T for $R=10$ nm are due to the singlet $\leftrightarrow$ triplet transitions (see Fig. 2). Because during the transitions there is conservation of total spin, we must have $\Delta S=0$, which implies that the allowed final states also change when the spin state of the ground state changes. This is responsible for the discontinuities in the transition energies as a function of the magnetic field. Such discontinuities are not predicted in the case of parabolic quantum dots. Therefore, this would be a clear signature of the hard-wall nature of the confinement potential in a cyclotron resonance experiment.

In Ref. 8, the cyclotron resonance energy was measured for $In_xGa_{1-x}As/GaAs$ quantum disks of a diameter about 20 nm and a thickness of about 4.5 ML. We have applied our theoretical results to this experimental system and found that good agreement could be obtained (see Fig. 7) for a radius of $R\approx 12$ nm, where we assumed a thickness of $L_z=2.5$ nm. In Fig. 7 we show the results for one electron (dashed curve) and two electrons with $\lambda=0$ (dotted curve) in the electron-electron interaction potential $V_c(\rho)$, which implies zero width of the disk for the Coulomb interaction, and includes the finite width of the disk in the Coulomb repulsion potential (full curve). Here we used $\lambda=0.4$ nm. Notice that the finite width of the disk has practically no influence on the Coulomb contribution to the transition energy. It slighty decreases it. Drexler *et al.*[8] fitted their transition energies to a parabolic confinement potential with $\hbar\omega_0=41$ meV and used a mass of $m^*/m_0=0.07$, which is that of GaAs. The agreement with the experimental data was as good as shown in Fig. 7. The reason for this can be traced back to the strong confinement, which results in an almost pure linear dependence of the transition energy on the magnetic field strength. For the experimental magnetic field range this is the case and such a behavior does not depend on the type of confinement potential. Only for higher magnetic fields (see Fig. 6) are differences in ΔE between the two types of confinement expected, like jumps in ΔE when the system makes a transition from a singlet to a triplet state. Furthermore, in the hard-wall confinement case, it should also be possible to observe more transitions (see Figs. 5 and 6).

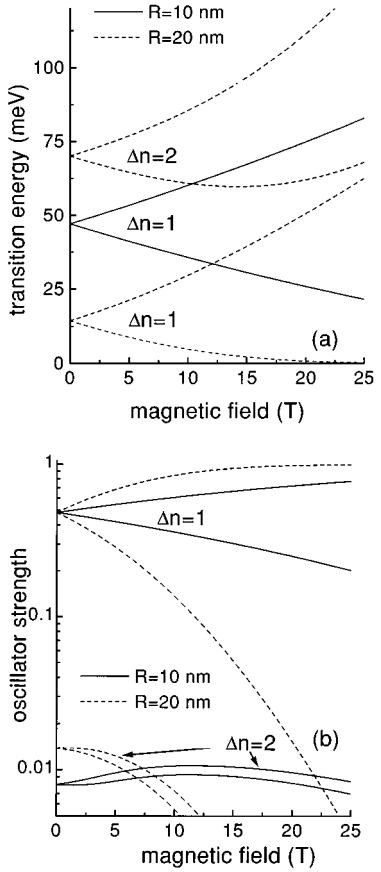

FIG. 5. (a) The allowed one-electron transition energies as function of the magnetic field, and (b) the corresponding oscillator strengths for the disks of Fig. 1.

V. CONCLUSIONS

The energy levels, the electron density, the pair correlation function, the cyclotron transition energies, and the corresponding oscillator strengths were calculated for quantum disks containing one or two electrons. The quantum disk with radius R has a nonzero thickness L_z and the confine-

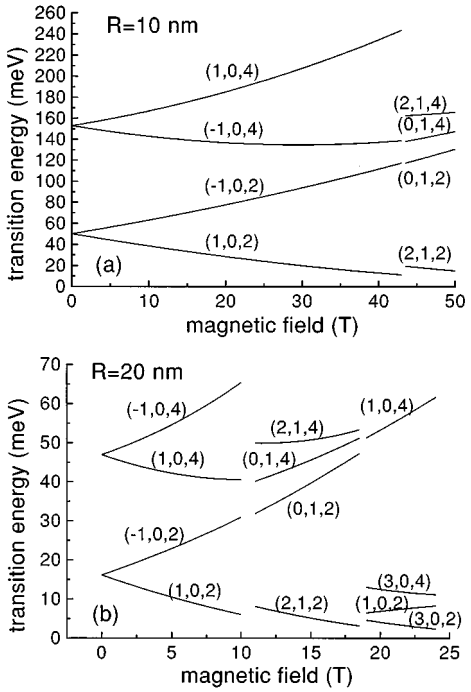

FIG. 6. The cyclotron transition energies for a two-electron disk of radius (a) $R=10$ nm and (b) $R=20$ nm. The transition energies are labeled by their final states (L,S,N).

ment potential is of the hard-wall type with finite height. We showed that for $L_z \ll R$, the adiabatic approximation is applicable and the three-dimensional quantum problem can be reduced to an effective two-dimensional one.

We are able to describe the cyclotron resonance data of Ref. 8 reasonably well, without using any fitting parameters. In the present hard-wall situation, we predict that the cyclotron resonance transition energy exhibits jumps each time the ground state energy undergoes a singlet $\leftrightarrow$ triplet transition. Futhermore, more transitions are possible (although with small oscillator strength) than in the case of parabolic confinement, due to the lifting of the $\Delta N=1$ selection rule. The latter is a consequence of the fact that in the present system,

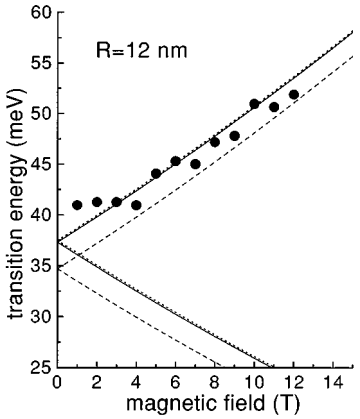

FIG. 7. The cyclotron transition energy for an $In_xGa_{1-x}As$ disk of radius $R=12$ nm and thickness $L_z=2.5$ nm, which is embedded in GaAs. We show the one-electron result (dashed curve), the two-electron result including (full curve) and excluding (dotted curve) the finite width of the disk in the Coulomb energy.

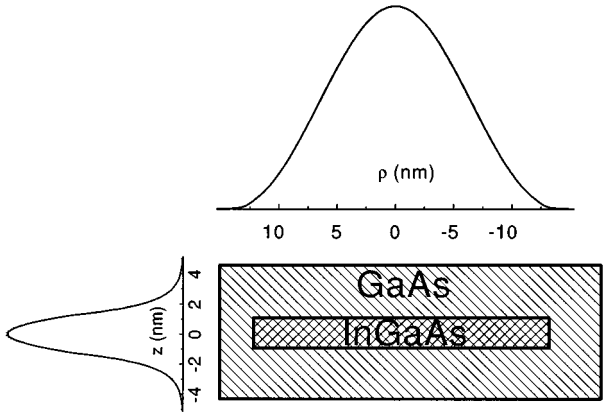

FIG. 8. Side view of the disk together with the electron probability distribution along the $(\rho,z=0)$ and the $(\rho=0,z)$ directions.

radiation is also able to couple with other degrees of freedom than the center of mass motion of the electrons.

ACKNOWLEDGMENTS

This work was supported by the Belgian National Science Foundation (NFWO), the Interuniversity Microelectronics Center (IMEC, Leuven), INTAS-93-1495, and the Russian Foundation for Fundamental Investigations 95-022-04704-a.

APPENDIX

Let us consider the three-dimensional one-electron problem without magnetic field,

$$\left[-\vec{\nabla}\frac{\hbar^2}{2m(\vec{r})}\vec{\nabla}+V(\vec{r})\right]\Psi(\vec{r})=E\Psi(\vec{r}), \tag{A1}$$

where the confining potential $V(\vec{r})$ is equal to zero inside the disk ($\rho<R, |z|<L_z/2$), with R the radius of the quantum disk and L_z its thickness. Outside the disk the confining potential is $V(\vec{r})=V_0$. Because of the finite value of the barrier height, V_0, the eigenvalue problem (A1) cannot be solved exactly.

We consider the ground state, which does not depend on the axial angle, $\Psi_0(\vec{r})=\Psi_0(z,\rho)$, and, consequently, the problem is reduced to a 2D one. Equation (A1) was put on a space grid and we used the inverse iteration technique in order to obtain the ground state energy E_0 and the ground state wave function $\Psi_0(z,\rho)$. Figure 8 shows the one-electron density distribution $|\Psi_0(z,\rho)|^2$ for the ground state along $(z=0,\ \rho)$ and perpendicular $(z,\rho=0)$ to the disk for a $In_xGa_{1-x}As$ disk with radius $R=12$ nm, which is imbedded in GaAs. The width of the quantum disk was $L_z=2.5$ nm, with $m_1=0.041$ ($In_xGa_{1-x}As$), $m_2=0.067$ (GaAs), and barrier height $V_0=500$ meV. We found for the energy of the ground state 277.9 meV.

Due to the large difference in the radial and longitudinal dimensions of the disk, one can use an adiabatic approach and assume that there is no coupling between the electron motion in the (x,y) plane and in the z direction. First, we consider the motion in the z direction, where we have the strongest confinement. This is a one-dimensional quantum

well problem. The wave function of the ground state has a simple form inside $\phi_0(z)=\phi_1(|z|<L_z/2)=\cos(\kappa_1 z)$ and outside $\phi_0(z)=\phi_2(|z|>L_z/2)=\exp(-\kappa_1|z|)$ the well, where $\kappa_1=\sqrt{2m_1E_0/\hbar}$, $\kappa_2=\sqrt{2m_1(V_0-E_0)/\hbar}$. Using the conditions for continuity of the wave function and its first derivative, $\phi_1(|z|=L_z/2)=\phi_2(|z|=L_z/2)$, $\kappa_1\phi_1(|z|=L_z/2)/m_1=\kappa_2\phi_2(|z|=L_z/2)/m_2$, we obtain the transcendental equation $\tan(\kappa_1 L_z/2)=m_1\kappa_2/m_2\kappa_1$, which determines the energy of the ground state in the 1D well. For $L_z=2.5$ nm, $m_1=0.041$, $m_2=0.067$, and $V_0=500$ meV, the energy of the ground state is $E_0^{1D}=254.8$ meV. Now we assume that the wave function for the three-dimensional problem can be written as $\Psi(\vec{r})=\phi_0(z)\Psi(\vec{\rho})$, where $\phi_0(z)$ is the wave function of the above 1D well and $\vec{\rho}=(x,y)$. Substituting this expression in the Schrödinger equation and integrating out the z coordinates by taking the average $\langle\phi_0(z)|H|\phi_0(z)\rangle=H^{2D}$, we obtain the effective one-electron Hamiltonian,

$$H^{2D}=\vec{p}\frac{1}{2m'(r)}\vec{p}+V'(\rho), \tag{A2}$$

where $\vec{p}=i\hbar\vec{\nabla}$, $V'(\rho)=V(\rho)-E_0^{1D}$, $m_2'=m_2$, and

$$\frac{1}{m_1'}=\frac{1}{m_1}\int_0^{L_z/2}\phi_0^2(z)dz+\frac{1}{m_2}\int_{L_z/2}^{\infty}\phi_0^2(z)dz. \tag{A3}$$

For $L_z=2.5$ nm, we obtain $m_1'=0.0465$, with $V'=245.2$ meV. Thus, incorporating the z motion of the electron leads to an effective increase of the electron mass inside the disk and an effective lowering of the potential barrier. The energy of the ground state of the Hamiltonian (A2) is $E_0^{2D}=22.6$ meV for $R=12$ nm. Thus, using the adiabatic approximation we add the zero-point energies in the z direction (E^{1D}) with the one in the (x,y) plane (E^{2D}) and find that the ground state energy of the 3D problem is $E_0=E^{1D}+E^{2D}=277.4$ meV. We stress that the 2D (x,y) problem is not independent from the 1D z problem, because it contains (1) the barrier lowering, $V\rightarrow V'$ and (ii) the effective mass increase, $m\rightarrow m_1'$, because of the z-motion penetration of the electron into the barrier. This result compares very well with the result 277.9 meV obtained from our pure numerical solution of Eq. (A1). The binding energy is thus $\Delta E=500$ meV -277.4 meV $=222.6$ meV.

*Electronic address: peeters@uia.ua.ac.be

†Permanent address: Institute of Theoretical and Applied Mechanics, Russian Academy of Sciences, Novosibirsk 630090, Russia.

[1] For a recent review see, e.g., N.F. Johnson, J. Phys. Condens. Matter **7**, 965 (1995).

[2] M.A. Kastner, Phys. Today **46** (1), 24 (1993); D. Heitmann and J.P. Kotthaus, *ibid.* **46** (6), 56 (1993).

[3] D. Leonard, M. Krishnamurthy, C.M. Reaves, S.P. Denbaars, and P.M. Petroff, Appl. Phys. Lett. **63**, 3203 (1993).

[4] R. Nötzel, T. Fukui, and H. Hasegawa, Appl. Phys. Lett. **65**, 2854 (1994).

[5] J. Oshinowo, M. Nishioka, S. Ishida, and Y. Arakawa, Appl. Phys. Lett. **65**, 1421 (1994).

[6] M. Grundmann, N.N. Ledentsov, R. Heitz, L. Eckey, J. Chisten, J. Böhrer, D. Bimberg, S.S. Ruvimov, P. Werner, U. Richter, J. Heydenreich, V.M. Ustinov, A.Yu. Egorov, A.E. Zhukov, P.S. Kopev, and Zh.I. Alferov, Phys. Status Solid B **188**, 249 (1995); D. Leonard, K. Pond, and P.M. Petroff, Phys. Rev. B **50**, 11 687 (1994); G. Medeiros-Ribeiro, D. Leonard, and P.M. Petroff, Appl. Phys. Lett. **66**, 1767 (1995).

[7] S. Fafard, D. Leonard, J.L. Merz, and P.M. Petroff, Appl. Phys. Lett. **65**, 1388 (1994).

[8] H. Drexler, D. Leonard, W. Hansen, J.P. Kotthaus, and P.M. Petroff, Phys. Rev. Lett. **73**, 2252 (1994).

[9] L. Brey, N.F. Johnson, and B.I. Halperin, Phys. Rev. B **40**, 10 647 (1989); P.A. Maksym and T. Chakraborty, Phys. Rev. Lett. **65**, 108 (1990); F.M. Peeters, Phys. Rev. B **42**, 1486 (1990).

[10] U. Rössler, D.A. Broido, and F. Bolton, in *Low Dimensional Electronic Systems: New Concepts*, edited by G. Bauer, F. Kuchar, and H. Heinrich (Springer-Verlag, Berlin, 1992), p. 21.

[11] D. Pfannkuche and R.R. Gerhardts, Phys. Rev. B **44**, 13 132 (1991); T. Chakraborty, V. Halonen, and P. Pietlainen, *ibid.* **43**, 14 289 (1991); X.C. Xie, S. Das Sarma, and S. He, *ibid.* **48**, 8454 (1993).

[12] F. Geerinckx, F.M. Peeters, and J.T. Devreese, J. Appl. Phys. **68**, 3435 (1990).

[13] G.W. Bryant, Phys. Rev. B **31**, 7812 (1985).

[14] M. Krijn, Semicond. Sci. Technol. **6**, 27 (1991); S. Tiwari and D.J. Frank, Appl. Phys. Lett. **60**, 630 (1992).

[15] A. Matulis and F.M. Peeters, J. Phys. Condens. Matter **6**, 7751 (1994).

[16] R. Price, X. Zhu, S. Das Sarma, and P.M. Platzman, Phys. Rev. B **51**, 2017 (1995).

[17] M. Wagner, U. Merkt, and A.V. Chaplik, Phys. Rev. B **45**, 1951 (1992).

[18] R.C. Ashoori, H.L. Störmer, J.S. Weinger, L.N. Pfeiffer, K.W. Baldwin, and K.W. West, Phys. Rev. Lett. **71**, 613 (1993); **68**, 3088 (1992); P. Hawrylak, *ibid.* **71**, 3347 (1993).

[19] U. Merkt, J. Huser, and M. Wagner, Phys. Rev. B **43**, 7320 (1991); D. Pfannkuche, V. Gudmundsson, and P.A. Maksym, *ibid.* **47**, 2244 (1993); J.-J.S. De Groote, J.E.M. Hornos, and A.V. Chaplik, *ibid.* **49**, 12 773 (1992); M. Wagner, U. Merkt, and A. Chaplik, *ibid.* **45**, 1951 (1992).

[20] B. Adolph, S. Glutsch, and F. Bechstedt, Solid State Electron. **37**, 1149 (1994).